

Figure 10. Examples of correctly predicted images with their prediction heatmaps for "Overall percent of abnormal volume" parameter:

- a) patient ID 13676, actual value 14
- b) patient ID 2641, actual value 30
- c) patient ID 19415, actual value 34

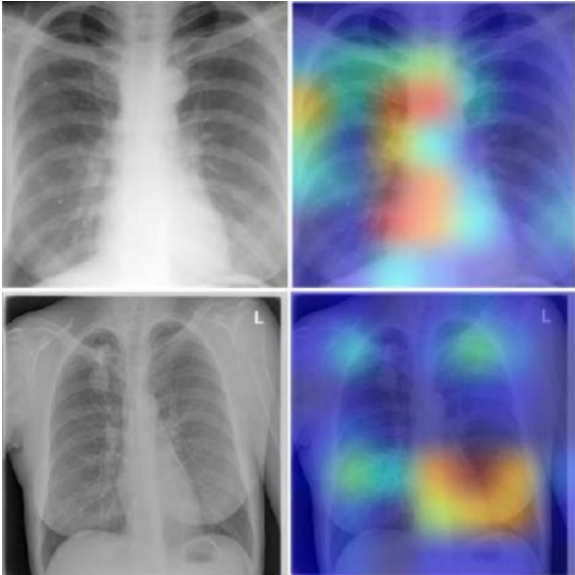


Figure 11. Examples of incorrectly predicted "Overall percent of abnormal volume" with corresponding prediction heatmaps.

but "Overall percent of abnormal volume" parameter is set to zero.



Figure 12. The patient's right lung has been damaged, but "Overall percent of abnormal volume" parameter is set to zero.

A study of patient ID 426 in the CASE BROWSER [2] found that the other parameter "Pleural Effusion. of hemithorax involved" is equal to 50 sextants were annotated and have some lesions: Upper, Middle, Lower Right and Lower Left Sextants. The right lung is particularly badly damaged.

At least 44 such images with markup inconsistencies were found. It is necessary to exclude them from the training samples.

*Simple consistency checks* between different CXR annotation markup parameters should be developed for future research. It is necessary to pay attention not only to the images, but also to the various textual descriptions provided.

As a result, it was concluded that the high MAE value is due to the following reasons:

- background noise (outside the lungs) that requires mask cropping to remove it;
- the presence of artifacts in the lungs that requires more data to train the neural network to correctly distinguish these artifacts;
- some errors in CXR image annotations that should be excluded from the dataset.

## VII. Discussion of the application of semantic technologies in the context of the tasks considered in this paper

In 1982, Japanese scientists developed a program for the fifth generation of electronic computing machines. Despite the fact that more than 42 years have passed, the fifth generation computers have not been fully realized. The main difficulty in creating fifth-generation computers or future computers is to create a machine with artificial intelligence (AI) that will be able to draw logical conclusions from the facts presented.

To interact with a fifth-generation computer, a person (user) will not need to develop software for the machine

to solve the task at hand. In addition, fifth generation computers will solve the problem of data formalization in the interaction between computer and computer and human and computer. Commands for the machine can be formulated in ordinary spoken language without knowledge of formal programming languages as well as input and output data formats.

Thus, fifth-generation computers are intelligent semantic systems with extremely high interoperability. Interoperability is the ability of a product or system, whose interfaces are completely open, to interact and function with other products or systems without any access or implementation restrictions.

Although fifth generation computers have not yet been realized, active work is being done to remove the barriers between humans and computers, and between computers and computers.

One of the directions for the development of interoperable intelligent computer systems is automatic data transformation between different modalities: image to text, text to image, speech to text, text to speech, image to speech, speech to image, image to music, 3D reconstruction of an object from a set of images, CT scan to X-ray image, satellite image to geographical map, geographical map to satellite image and other modality transformations [19], [20].

This research project is developing an intelligent semantic system that converts a textual description into an image, namely the textual markup of a radiologist into a heatmap of lesion foci in the corresponding CXR medical image.

A neural network trained to solve such a problem will be a decision support system for population screening. The trained neural network model will produce a textual description of lung lesions based on the patient's chest radiograph, as well as a heatmap corresponding to these lesions in the form of a graphical representation Fig.13.



Figure 13. Operation schematic of the CXR-based decision support system under development.

The problem of generating a heatmap from a textual description and the subsequent problem of generating a heatmap and corresponding textual description from an input CXR image is one of the challenges of semantic image segmentation.

Semantic image segmentation is the task of dividing parts of an image into subgroups of pixels belonging to corresponding objects, with subsequent classification of these objects. Unlike classification and object detection tasks, the

task of semantic segmentation is more complex both in terms of solution methods and computational resources [21].

Analyzing the literature to identify different semantic methods for medical image processing revealed the following approaches:

- probabilistic latent semantic analysis (PLSA), which, in conjunction with neural network, is able to mining the hidden semantics of an image [22];
- implementation of Semantic Similarity Graph Embedding (SSGE) framework, which explicitly explores the semantic similarities among images [23];
- investigation and development of the concept of a personal intellectual assistant (secretary, referent) [24].

Unfortunately, this paper does not apply the found semantic methods to medical image processing. However, the application of such semantic techniques in the context of the tasks considered in this paper is very relevant in future investigations.

As correctly noted in [25], "Currently, decision support systems in radiation mammology focus on the detection and classification of neoplasms, despite the fact that *the real work of a radiologist does not imply a diagnosing*. Computer vision systems use a *black box model* and do not explain the results of work, which is unacceptable in medicine".

This study also focuses on a deeper evaluation of the behavior of such a "black box"(neural network model) by studying the activation heatmaps on different convolutional layers of the neural network, which are obtained using the Gradient-weighted Class Activation Mapping (Grad-CAM) method [18]. The investigation of heatmaps on different convolutional layers provides a better understanding of the decision-making logic of the neural network based on the input data.

Fig. 5 shows the result of the semantic analysis of lesion names. As shown in Fig. 5, there are four classes of lesions: "Cavity" "Density" "Nodule" and "Collapse". Meanwhile, the two classes "Density" and "Nodule" have meaning overlap in the three lesion names. In the future, semantic analysis methods will be applied to better understand the disease asymmetry of different lung lobes (see Tab. II).

After the decision support system for population screening is completed, it is planned to be implemented into the already existing software "AI-based software for computer-assisted diagnosis of lung diseases using chest X-Ray and CT images"(LungExpert, <https://lungs.org.by>).

## VIII. Conclusions

In this article, text annotations to CXR images were analyzed. At this stage of the project, the main efforts of the authors were focused on the formation of databases

for further research. A catalogue tree with new datasets is described and constantly developing.

Two main tasks based on radiologists' textual annotations were planned and the corresponding pipeline for the neural

networks training was described: pulmonary disease study using sextants and the pulmonary disease study using overall characteristics.

The task of predicting the parameter "Overall percent of abnormal volume" showed that it is necessary to develop additional simple consistency checks between different CXR textual annotations. Also using lung masks is a good idea to improve the quality of neural networks. Further research is planned to create neural network attention heatmaps based on the textual descriptions of radiologists.

#### Acknowledgment

This work was carried out with the financial support of the ISTC-PR150 "Belarus TB Database and TB Portal" project.

#### Reference

- [1] TB Portals. Available at: <https://tbportals.niaid.nih.gov> (accessed 2024, March)
- [2] CASE BROWSER. Available at: <https://data.tbportals.niaid.nih.gov> (accessed 2024, March)
- [3] TB DEPOT. Available at: <https://depot.tbportals.niaid.nih.gov/cohort-creation?tab=4> (accessed 2024, March)
- [4] Tuberculosis (pulmonary manifestations). Available at: <https://radiopaedia.org/articles/tuberculosis-pulmonarymanifestations-1> (accessed 2024, March)
- [5] Statistical Atlas of Lung Lesions. Available at: <https://image.org.by/lesionAtlas> (accessed 2024, March)
- [6] V. Kovalev, V. Liauchuk, A. Gabrielian, A. Rosenthal, "Towards Statistical Atlas of Lung Lesions," *International Journal of Computer Assisted Radiology and Surgery*, 21-25 June, Munich, Germany, 2020, Vol. 15, Suppl. 1, pp. s31-s32. [Online]. Available: <https://www.researchgate.net/publication/344217581>
- [7] D.M. Hansell, A.A. Bankier, H. MacMahon, T.C. McLoud, Towards Statistical Atlas of Lung Lesions
- [8] Lung cavity. Available at: [https://en.wikipedia.org/wiki/Lung\\_cavity](https://en.wikipedia.org/wiki/Lung_cavity) (accessed 2024, March)
- [9] D.M. Hansell, A.A. Bankier, H. MacMahon, T.C. McLoud, N.L. Müller, J. Remy, et al., "Fleischner Society: Glossary of terms for thoracic imaging," *Radiology*, 2008, Vol. 246, No. 3, pp. 697-722. [Online]. Available: <https://doi.org/10.1148/radiol.2462070712>
- [10] D.M. Hansell, A.A. Bankier, H. MacMahon, T.C. McLoud, K. Loverdos, A. Fotiadis, C. Kontogianni, M. Iliopoulou, M. Gaga, "Lung nodules: A comprehensive review on current approach and management," *Annals of Thoracic Medicine*, 2019, Vol. 14, Issue 4, pp. 226-238. [Online]. Available: <https://www.ncbi.nlm.nih.gov/pmc/articles/PMC6784443>
- [11] D.M. Hansell, A.A. Bankier, H. MacMahon, T.C. McLoud, G. Metry, G. Wegenius, B. Wikström, V. Källskog, P. Hansell, P.G. Lindgren, H. Hedenström, B.G. Danielson, "Lung density for assessment of hydration status in hemodialysis patients using the computed tomographic densitometry technique," *Kidney international*, 1997, Vol. 52, Issue 6, pp. 1635-1644. [Online]. Available: <https://doi.org/10.1038/ki.1997.496>
- [12] D.M. Hansell, A.A. Bankier, H. MacMahon, T.C. McLoud, Pulmonary infiltrate. Available at: [https://en.wikipedia.org/wiki/Pulmonary\\_infiltrate](https://en.wikipedia.org/wiki/Pulmonary_infiltrate) (accessed 2024, March)
- [13] D.M. Hansell, A.A. Bankier, H. MacMahon, T.C. McLoud, Collapsed Lung (Pneumothorax). Available at: <https://www.pennmedicine.org/for-patients-and-visitors/patient-information/conditions-treated-at-to-z/collapsed-lung-pneumothorax> (accessed 2024, March).
- [14] 'Timika score' on x-rays may help identify complex TB cases. Available at: <https://www.auntminnie.com/imaginginformatics/artificial-intelligence/article/15635618/timika-score-on-x-rays-may-help-identify-complex-tb-cases> (accessed 2024, March)
- [15] A. Chakraborty, A.J. Shivananjanaiyah, S. Ramaswamy, N. Chikkavenkatappa, "Chest X ray score (Timika score): an useful adjunct to predict treatment outcome in tuberculosis," *Advances in Respiratory Medicine*, 2018, Vol. 86, No. 5, pp. 205-210. [Online]. Available: <https://doi.org/10.5603/ARM.2018.0032>
- [16] LungExpert. Available at: <https://lungs.org.by> (accessed 2024, March).
- [17] TB DEPOT Data Dictionary. Available at: <https://depot.tbportals.niaid.nih.gov/data-dictionary> (accessed 2024, March)
- [18] ImageNet. Available at: <https://www.image-net.org> (accessed 2024, March)
- [19] R.R. Selvaraju, M. Cogswell, A. Das, R. Vedantam., D. Parikh, D. Batra, "Grad-CAM: Visual Explanations from Deep Networks via Gradient-Based Localization," *International Journal of Computer Vision*, 2020, Vol. 128, No. 2, pp. 336-359. [Online]. Available: <https://doi.org/10.1007/s11263-019-01228-7>
- [20] Top 7 text-to-image generative AI models. Available at: <https://byby.dev/ai-text-to-image-models> (accessed 2024, Apr)

- [21] Rohit Kundu. Image Processing: Techniques, Types, & Applications [2023]. Available at: <https://www.v7labs.com/blog/imageprocessing-guide> (accessed 2024, Apr).
- [22] M. Arsalan, M. Owais, T. Mahmood, J. Choi, K.R. Park, "Artificial Intelligence-Based Diagnosis of Cardiac and Related Diseases," *Journal of Clinical Medicine*, 2020, 9(3):871, pp 1–27. [Online]. Available: <https://doi.org/10.3390/jcm9030871>
- [23] M.R. Zare, M. Mehtarizadeh, "An Ensemble of Deep Semantic Representation for Medical X-ray Image Classification," *2021 55th Annual Conference on Information Sciences and Systems (CISS)*, Baltimore, MD, USA, 2021, pp. 1–6. [Online]. Available: <https://www.doi.org/10.1109/CISS50987.2021.9400268>
- [24] B. Chen, Z. Zhang, Y. Li, G. Lu, D. Zhang, "Multi-Label Chest X-Ray Image Classification via Semantic Similarity Graph Embedding," in *IEEE Transactions on Circuits and Systems for Video Technology*, April 2022, vol. 32, no. 4, pp. 2455–2468. [Online]. Available: <https://www.doi.org/10.1109/TCSVT.2021.3079900>
- [25] V. Rostovtsev, "Intelligent health monitoring systems," *Otkrytye semanticheskie tekhnologii proektirovaniya intellektual'nykh system* [Open semantic technologies for intelligent systems], 2023, pp. 237–240. [Online]. Available: <https://libeldoc.bsuir.by/handle/123456789/51289>
- [26] A. Kayeshko, A. Efimova, "Decision support system for breast cancer screening," *Otkrytye semanticheskie tekhnologii proektirovaniya intellektual'nykh system* [Open semantic technologies for intelligent systems], 2021, pp. 229–232. [Online]. Available: <https://libeldoc.bsuir.by/handle/123456789/45424>

## ОБРАБОТКА РЕНТГЕНОВСКИХ ИЗОБРАЖЕНИЙ ГРУДНОЙ КЛЕТКИ НА ОСНОВЕ ТЕКСТОВЫХ АННОТАЦИЙ РАДИОЛОГОВ

Косарева А. А., Павленко Д. А., Снежко Э. В.

Проанализировано более 11 000 рентгеновских снимков грудной клетки и соответствующих им текстовых аннотаций, а также проведены первые пилотные исследования по обработке изображений с учетом текстовых аннотаций специалистов-рентгенологов. Разработан конвейер обработки изображений для базы данных и нейронной сети. Проведено прогнозирование параметра «Общий процент аномального объема», для которого средняя абсолютная ошибка составила 11,073 при использовании нейросетевой модели InceptionResNet50V2.

Received 12.03.2024